nature cell biology

Regulation of Hippo pathway transcription factor TEAD by p38 MAPK-induced cytoplasmic translocation

Kimberly C. Lin[1], Toshiro Moroishi[1], Zhipeng Meng[1], Han-Sol Jeong[1,2], Steven W. Plouffe[1], Yoshitaka Sekido[3], Jiahuai Han[4], Hyun Woo Park[1,5,6] and Kun-Liang Guan[1,6]

The Hippo pathway controls organ size and tissue homeostasis, with deregulation leading to cancer. The core Hippo components in mammals are composed of the upstream serine/threonine kinases Mst1/2, MAPK4Ks and Lats1/2. Inactivation of these upstream kinases leads to dephosphorylation, stabilization, nuclear translocation and thus activation of the major functional transducers of the Hippo pathway, YAP and its paralogue TAZ[1,2]. YAP/TAZ are transcription co-activators that regulate gene expression primarily through interaction with the TEA domain DNA-binding family of transcription factors (TEAD)[3]. The current paradigm for regulation of this pathway centres on phosphorylation-dependent nucleocytoplasmic shuttling of YAP/TAZ through a complex network of upstream components[2]. However, unlike other transcription factors, such as SMAD, NF-κB, NFAT and STAT, the regulation of TEAD nucleocytoplasmic shuttling has been largely overlooked. In the present study, we show that environmental stress promotes TEAD cytoplasmic translocation via p38 MAPK in a Hippo-independent manner. Importantly, stress-induced TEAD inhibition predominates YAP-activating signals and selectively suppresses YAP-driven cancer cell growth. Our data reveal a mechanism governing TEAD nucleocytoplasmic shuttling and show that TEAD localization is a critical determinant of Hippo signalling output.

We set out to identify signals that may regulate TEAD subcellular localization by focusing on conditions known to inhibit YAP/TAZ such as serum starvation[4], energy stress by glucose starvation[5,6], PKA activation by forskolin[4], disruption of the actin cytoskeleton by latrunculin B[7,8], Src inhibition by dasatinib[9] and inhibition of mevalonate synthesis by cerivastatin[10]. These well-known YAP/TAZ inhibitory stimuli indeed induced YAP/TAZ cytoplasmic localization, but failed to alter TEAD subcellular localization (Fig. 1a). In contrast, environmental stresses such as osmotic stress, high cell density and cell detachment induced cytoplasmic translocation of TEAD and YAP/TAZ (Fig. 1b and Supplementary Fig. 1a,b), demonstrating that only a subset of signals that induce YAP/TAZ cytoplasmic localization are capable of driving TEAD cytoplasmic localization.

The p38 MAP kinase is activated by stress, including hyperosmotic conditions; therefore, we examined whether p38 plays a role in regulation of TEAD during stress. Treatment with p38 inhibitors (SB203580 or PH797840) blocked osmotic-stress-induced, but not high-density-induced, TEAD cytoplasmic localization, indicating that p38 is specifically involved in TEAD cytoplasmic translocation following osmotic stress (Fig. 1c and Supplementary Fig. 1c). Activation of p38 by ectopic expression of p38 and its upstream kinase MKK3 also induced cytoplasmic translocation of TEAD and this effect was blocked by p38 inhibitor treatment (Fig. 1d and Supplementary Fig. 1d). We predicted that all four isoforms of p38 may play compensatory roles as ablating TEAD translocation required concentrations of p38 inhibitor that were sufficient for inhibiting all p38 isoforms (Supplementary Fig. 1e). Deletion of p38α/β (p38 2KO) resulted in p38γ/δ upregulation and did not impede TEAD cytoplasmic translocation (Supplementary Fig. 1f,g), further supporting the pharmacological evidence that all four isoforms of p38 play a role in TEAD regulation. When all four p38 genes were deleted in the p38α/β/γ/δ knockout (KO) (p38 4KO) cells, TEAD localization was insensitive to osmotic stress and largely retained in the nucleus (Fig. 1e,f and Supplementary Fig. 1f,h). Under basal conditions, deletion of p38 had no effect on TEAD localization and marginally increased YAP–TEAD activity, indicating

[1]Department of Pharmacology and Moores Cancer Center, University of California San Diego, La Jolla, California 92093, USA. [2]Division of Applied Medicine, School of Korean Medicine, Pusan National University, Yangsan, Gyeongnam 626-870, Republic of Korea. [3]Division of Molecular Oncology, Aichi Cancer Center Research Institute, 1-1 Kanokoden, Chikusa-ku, Nagoya, Aichi 464-8681, Japan. [4]State Key Laboratory of Cellular Stress Biology, Innovation Center for Cell Signaling Network, School of Life Sciences, Xiamen University, Xiamen, Fujian 361005, China. [5]Department of Biochemistry, College of Life Science and Biotechnology, Yonsei University, Seoul 03722, Republic of Korea.
[6]Correspondence should be addressed to H.W.P. or K.-L.G. (e-mail: hwp003@yonsei.ac.kr or kuguan@ucsd.edu)

Received 16 June 2016; accepted 21 June 2017; published online 28 July 2017; DOI: 10.1038/ncb3581

that p38 plays a role in regulation of TEAD mainly under conditions of cellular stress (Supplementary Fig. 1i,j). The specific role of p38 in osmotic stress is further supported by the result that p38 inhibition or knockout had no effect on density-induced TEAD cytoplasmic localization (Supplementary Fig. 1c). Collectively, the above observations demonstrate a critical role of p38 in stress-induced TEAD nucleocytoplasmic translocation. Consequently, TEAD cytoplasmic translocation by osmotic stress suppressed YAP/TAZ target gene expression induced by YAP-activating signals, such as lysophosphatidic acid (LPA) and serum[4], which was rescued by p38 inhibition (Fig. 1g,h). The NaCl-induced cytoplasmic localization of TEAD was slower than p38 phosphorylation and activation (Fig. 1i,j) but occurred concurrently with p38 dephosphorylation and cytoplasmic translocation (Fig. 1k). It is well established that post osmotic stress, p38 undergoes dephosphorylation and cytoplasmic translocation, indicating that TEAD cytoplasmic translocation occurs during the adaptation phase of stress response[11].

To further gain mechanistic insight into TEAD regulation by p38, we investigated the role of p38 protein–protein interaction and kinase activity, both of which are critically involved in p38 signal transduction[12]. We sought to determine whether p38 directly interacts with TEAD to promote cytoplasmic translocation. Interestingly, osmotic stress induced endogenous TEAD–p38 interaction, whereas serum-induced TEAD–YAP interaction was abolished by osmotic stress (Fig. 2a–c). In addition, exogenous p38 and MKK3 both showed interaction with TEAD (Fig. 2d). Using bacterially purified proteins in an *in vitro* binding assay, we show that TEAD can interact directly with p38 without scaffold proteins (Fig. 2e). Furthermore, p38 does not bind to YAP and thus regulates TEAD independently of YAP (Fig. 2f). The D domain, found in p38 binding partners, serves as a docking site for p38 protein–protein interactions[12]. We identified a putative D domain that is highly conserved within the TEAD family (Fig. 2g). Deletion of the D domain in TEAD abolished TEAD–p38 interaction (Fig. 2h). Consistently, p38 CD/ED, a p38 mutant that has lost its ability to interact with D-domain-containing substrates[13,14], significantly dampened TEAD–p38 interaction and was unable to induce TEAD cytoplasmic translocation (Fig. 2i–l). Ectopic expression of a kinase-deficient mutant, p38 KM, was also insufficient in binding to TEAD and driving cytoplasmic translocation (Fig. 2m,n). To determine whether TEAD cytoplasmic translocation is due to p38-mediated phosphorylation, we constructed TEAD4-4SP, in which the four putative p38 phosphorylation sites were mutated to alanine (Supplementary Fig. 2a). Using an *in vitro* kinase assay, we found TEAD4 to be a poor substrate for p38 phosphorylation with complete ablation of phosphorylation in the TEAD4-4SP mutant, indicating the absence of alternative phosphorylation sites (Supplementary Fig. 2b–d). Additionally, TEAD4-4SP displayed normal cytoplasmic translocation following osmotic stress (Supplementary Fig. 2e), suggesting that p38 kinase activity is required for TEAD interaction but does not directly phosphorylate TEAD to regulate its subcellular localization. Disruption of a putative TEAD nuclear export signal, as well as inhibition of chromosomal maintenance 1 (CRM1), a member of the importin family, using leptomycin B, largely ablated TEAD translocation, indicating that TEAD cytoplasmic translocation is an active, CRM1-mediated process (Supplementary Fig. 2f–h). In contrast to TEAD cytoplasmic localization, osmotic stress stimulates nuclear translocation of the transcription factor nuclear factor of activated T-cells 5 (NFAT5)[15]; thus, TEAD cytoplasmic translocation is a specific cellular response following osmotic stress (Supplementary Fig. 2i).

Next, we tested the effect of stress-induced TEAD cytoplasmic sequestration on YAP activation. Under osmotic stress, YAP-activating signals, such as serum and LPA, failed to induce YAP dephosphorylation and nuclear accumulation (Fig. 3a,b). ERK phosphorylation, however, was not affected, suggesting specificity of osmotic stress on YAP inhibition. Unexpectedly, stress evoked TEAD and YAP/TAZ cytoplasmic translocation in MAP4K 4/6/7, Mst1/2 and Lats1/2 KO cells, despite constitutively dephosphorylated YAP (Fig. 3c,d and Supplementary Fig. 3a–g). These results indicate that stress-induced TEAD and YAP/TAZ cytoplasmic retention is a Hippo-independent process and uncouples YAP dephosphorylation from its nuclear localization. Consistently, p38 inhibition restored TEAD in the nucleus in Lats1/2 KO cells (Fig. 3d). Compared with WT cells, p38 inhibition enhanced YAP/TAZ nuclear accumulation and target gene expression in the absence of Lats (Fig. 3d,e and Supplementary Fig. 3g). To test whether nuclear TEAD is required for YAP nuclear translocation following activating signals, we generated TEAD1/2/4 KO cells. YAP-activating signals promoted normal YAP dephosphorylation in the TEAD KO cells, but failed to elicit nuclear YAP/TAZ accumulation (Fig. 3f,g), suggesting that nuclear localization of TEAD is a prerequisite for proper YAP nuclear localization. No interaction was detected between YAP and p38, indicating that YAP cytoplasmic translocation is a consequence of TEAD regulation by p38 (Fig. 2f). Our data suggest that YAP nuclear localization is contingent on two conditions, dephosphorylation and nuclear localization of TEAD.

YAP is highly active in many cancers, particularly in uveal melanoma (UM) and mesothelioma, due to mutations in upstream components of the Hippo pathway[16–18]. YAP was constitutively hypophosphorylated and nuclear in the mesothelioma cells MSTO-211H (Lats2 mutation) and H2373 (NF2 mutation), even under YAP-inhibitory conditions (Fig. 4a,b and Supplementary Fig. 4a,b). However, osmotic stress promoted cytoplasmic translocation of both TEAD and YAP/TAZ, and consequently suppressed anchorage-independent growth (Fig. 4a–c and Supplementary Fig. 4a,b). Importantly, ectopic expression of a fusion of the TEAD DNA-binding domain to the VP16 transactivation domain, which is constitutively active and p38 binding deficient, restored colony-forming ability of mesothelioma cells (Fig. 4c–e and Supplementary Fig. 4c), suggesting that osmotic-stress-induced growth arrest is due to TEAD inhibition. To further examine whether stress-induced TEAD inhibition selectively suppresses YAP-driven cancer cell growth, we compared a series of UM cell lines with mutations in either GNAQ or BRAF. The GNAQ-mutant UM cells are YAP-dependent, while the BRAF-mutant UM cells are YAP-independent (Fig. 4f and Supplementary Fig. 4d,e)[17]. We observed that osmotic stress evoked p38-dependent cytoplasmic translocation of TEAD and YAP/TAZ in both 92.1 ($GNAQ^{Q209L}$) and OCM1 ($BRAF^{V600E}$) cells (Fig. 4g and Supplementary Fig. 4d–g). However, TEAD inhibition by osmotic stress or stable expression of p38 preferentially suppressed anchorage-independent growth of GNAQ-mutant UM cell lines, 92.1, OMM2.2, OMM2.3, Mel202, Mel270, but not BRAF-mutant UM

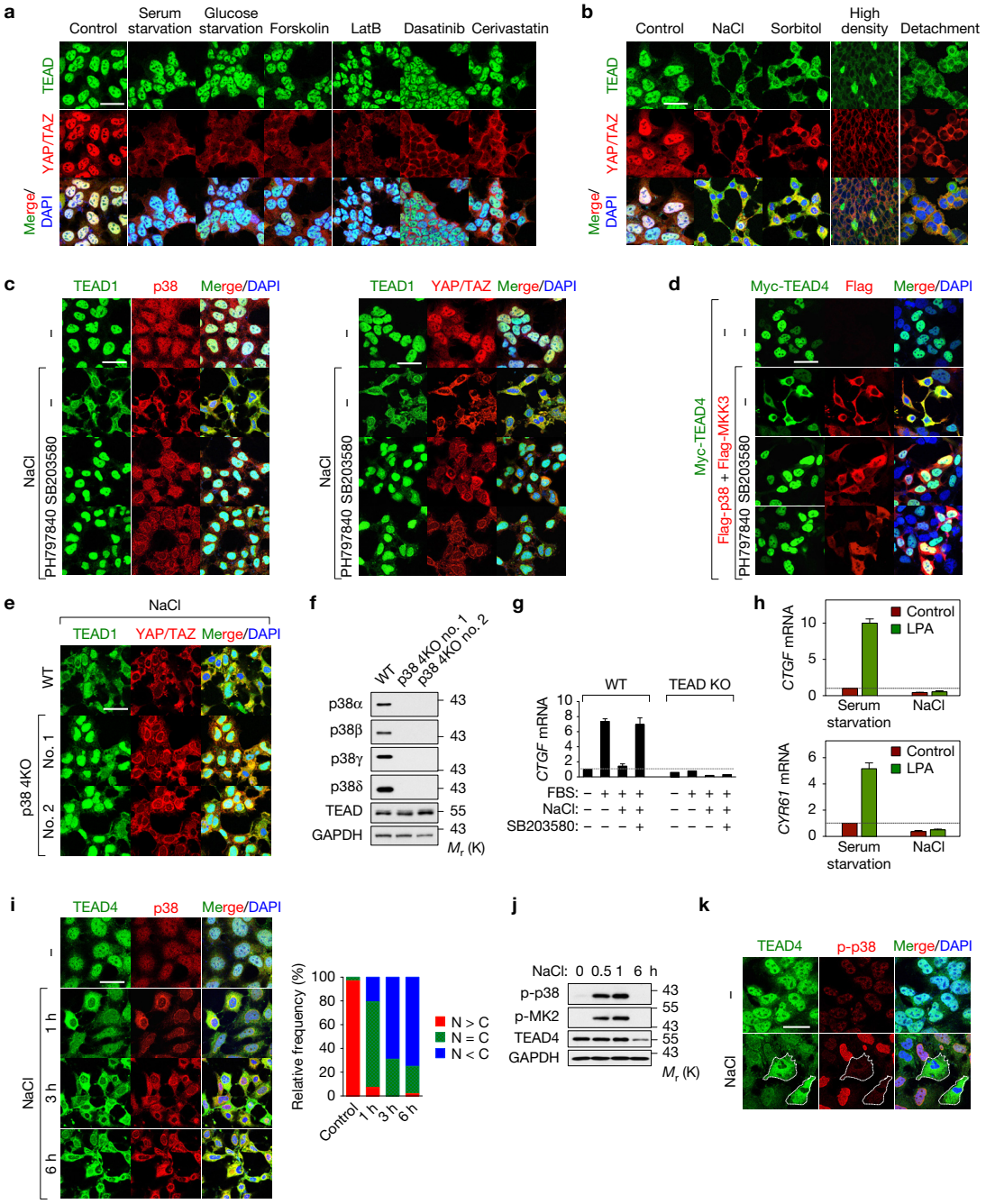

Figure 1 p38 mediates stress-induced TEAD cytoplasmic translocation. (**a**) Immunofluorescence staining of TEAD and YAP/TAZ in HEK293A cells treated with YAP-inhibiting signals. (**b**) Immunofluorescence detects TEAD cytoplasmic translocation by environmental stress. (**c**) Effect of p38 inhibitors on osmotic-stress-induced TEAD cytoplasmic translocation. HEK293A cells were pretreated with p38 inhibitors, and stimulated with NaCl and stained for immunofluorescence. (**d**) Ectopic expression of MKK3/p38 promotes TEAD4 cytoplasmic translocation. At 24 h after transfection, cells were treated with p38 inhibitors for 8 h and stained for immunofluorescence. (**e**) Immunofluorescence staining shows that deletion of p38 impairs TEAD nucleocytoplasmic shuttling by osmotic stress. Data for two independent p38 4KO clones are shown. (**f**) Western blotting of p38 isoforms in p38 4KO cells. (**g**) p38 mediates inhibition of YAP–TEAD target gene expression by stress. WT and TEAD KO cells were pretreated with NaCl and SB203580 as indicated, and then stimulated with 10% serum. *CTGF* mRNA expression was measured by qRT-PCR. Data are presented as mean ± s.e.m. from $n=3$ independent experiments. (**h**) Osmotic stress inhibits YAP–TEAD target gene expression. Cells were subject to serum starvation or NaCl, and then LPA-induced *CTGF* and *CYR61* mRNA expression was measured by qRT-PCR. Data are presented as mean ± s.e.m. from $n=3$ independent experiments. (**i**) Correlation between stress-induced cytoplasmic translocation of TEAD and p38. Cells were stimulated with NaCl for the indicated times and then subjected to immunofluorescence to detect p38. Quantification of TEAD nuclear localization (N) and cytoplasmic localization (C) is provided. Random views (~100 cells) were selected for quantification. (**j**) Time course of p38 activation by NaCl. Western blotting of phospho-p38 and its substrate phospho-MK2 following NaCl treatment. (**k**) Inverse correlation between stress-induced cytoplasmic translocation of TEAD and phospho-p38. Cells were stimulated with NaCl for 1 h and then subjected to immunofluorescence using a phospho-p38 antibody. Scale bars in **a**–**e**, **i** and **k** are 20 μm. Statistics source data are shown in Supplementary Table 1. Unprocessed original scans of blots are shown in Supplementary Fig. 5.

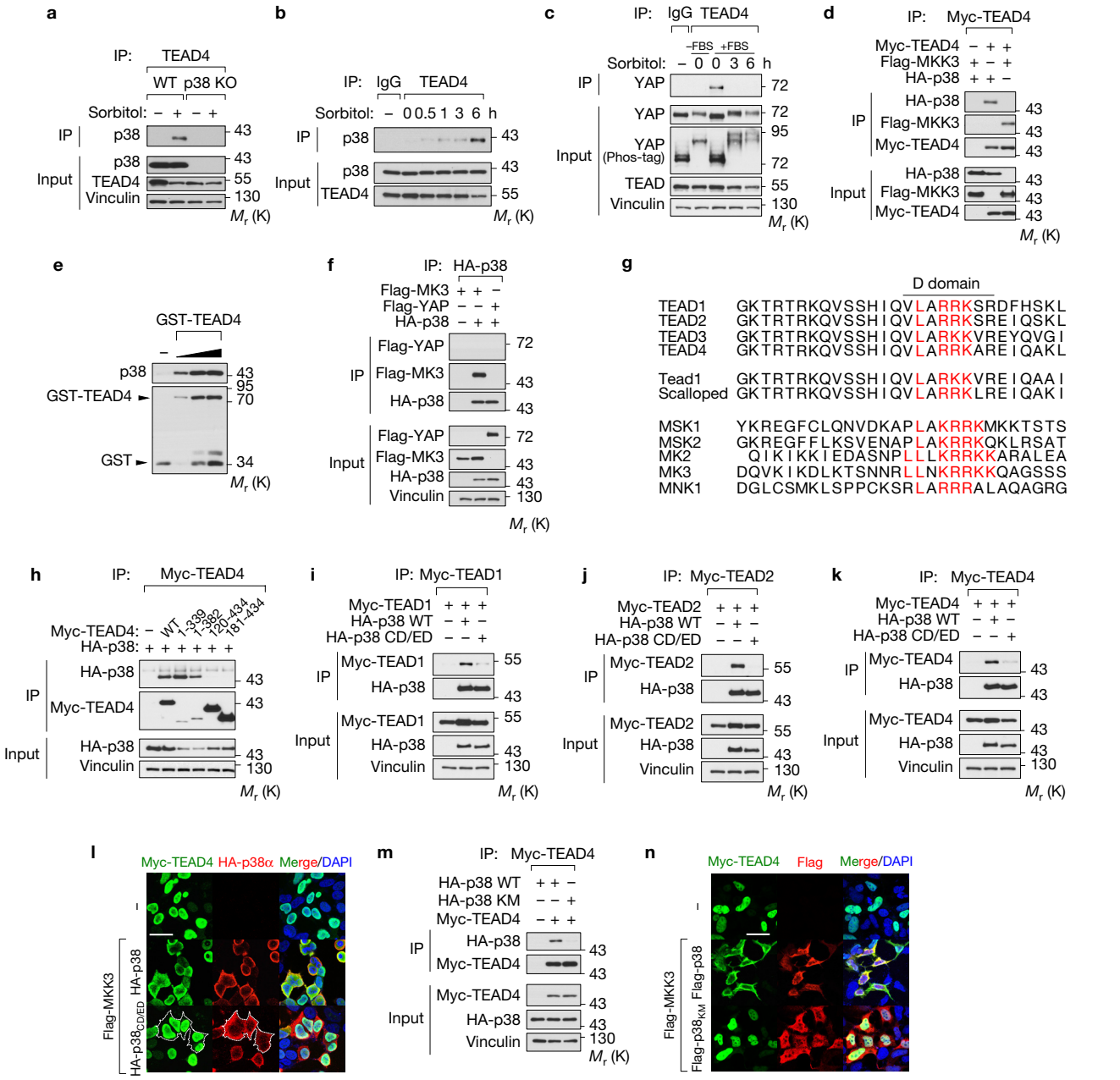

Figure 2 p38 mediates stress-induced TEAD cytoplasmic translocation via protein–protein interaction. (**a**) Detection of osmotic-stress-induced TEAD4 and p38 interaction by immunoprecipitation (IP) assay. (**b**) Immunoprecipitation showing time course of sorbitol-induced TEAD–p38 interaction. (**c**) TEAD immunoprecipitation shows that osmotic stress ablates TEAD–YAP interaction. (**d**) TEAD interacts with p38 and MKK3 as shown by immunoprecipitation. (**e**) *In vitro* binding assay using bacterially purified proteins shows a direct interaction between p38 and TEAD. (**f**) p38 does not interact with YAP. (**g**) Sequence alignment of TEAD with canonical p38 substrates. The putative D domain (red) is conserved in the amino terminus of all TEAD isoforms. (**h**) The TEAD D domain is required for interaction with p38. p38 binds TEAD4 carboxy-terminal truncation constructs (1–339 and 1–382), but not N-terminal truncations (120–434 or 181–434) in an immunoprecipitation assay. (**i**–**k**) The p38 CD/ED docking motif is required for interaction with TEAD. p38 WT, but not p38 CD/ED mutant, co-immunoprecipitates with TEAD1 (**i**), TEAD2 (**j**) and TEAD4 (**k**). (**l**) TEAD–p38 interaction mediates TEAD cytoplasmic translocation. Immunofluorescence staining shows that TEAD cytoplasmic translocation occurs in cells transfected with p38 WT, but not CD/ED mutant. (**m**) Effect of p38 kinase activity on p38–TEAD binding. Immunoprecipitation assay shows that TEAD binds p38 WT but not kinase-dead mutant, p38 KM. (**n**) Effect of p38 kinase activity on TEAD cytoplasmic translocation. Immunofluorescence shows that ectopic expression of p38 WT, but not kinase-dead mutant p38 KM, induces TEAD4 cytoplasmic translocation. Scale bars in **l** and **n** are 20 μm. Unprocessed original scans of blots are shown in Supplementary Fig. 5.

cell lines, OCM1 and OCM8 (Fig. 4h and Supplementary Fig. 4h). Consistently, TEAD translocation induced apoptosis specifically in the YAP-driven 92.1 cells but not the YAP-independent OCM1 cells (Fig. 4i). Furthermore, promotion of anchorage-independent growth by YAP-5SA transformation of MCF10A cells was also stunted by TEAD inhibition (Supplementary Fig. 4i). These results indicate

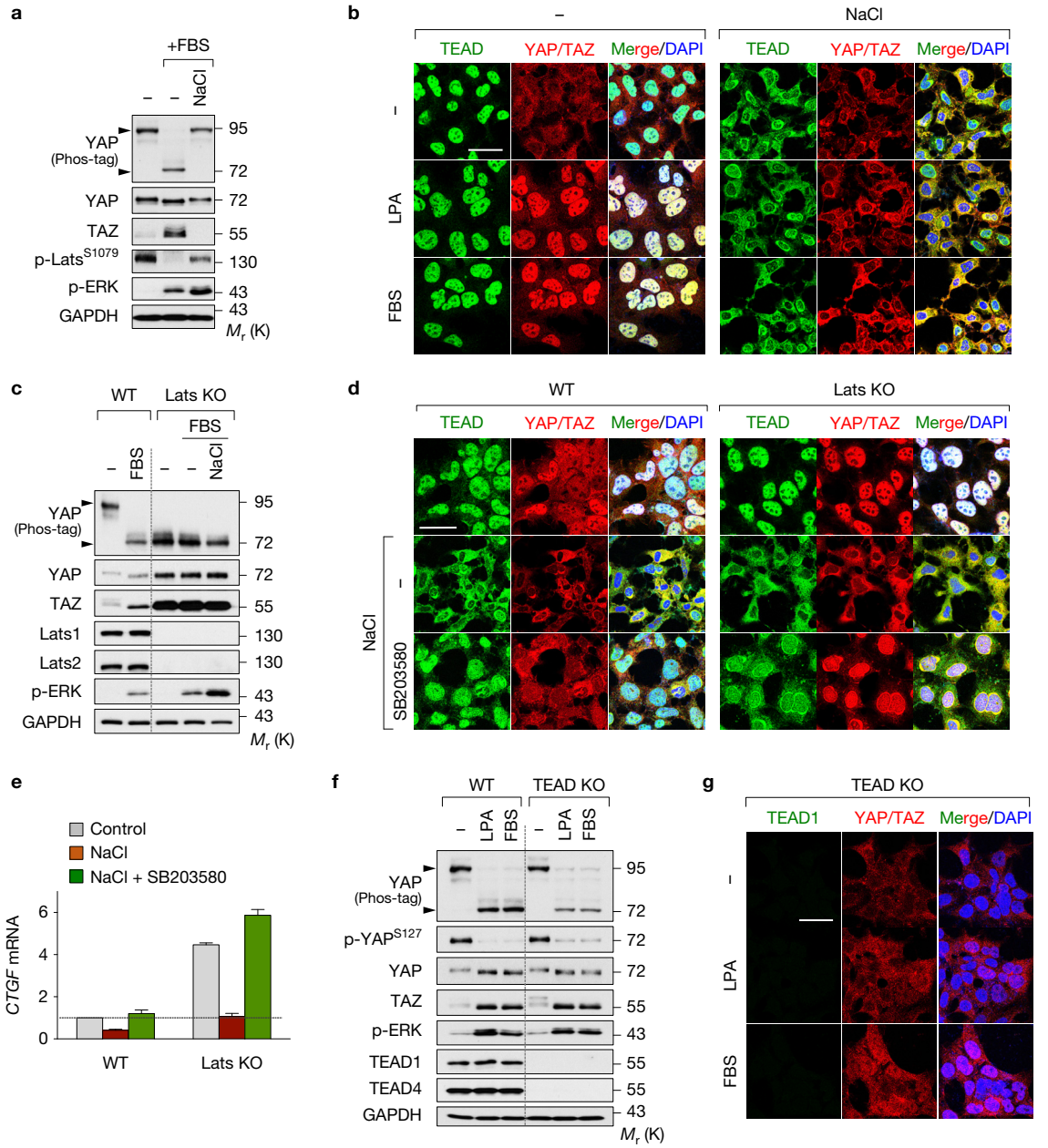

Figure 3 TEAD cytoplasmic translocation prevents YAP activation. (**a**,**b**) Effect of osmotic stress on serum- and LPA-induced YAP activation. Osmotic stress blocks serum- and LPA-induced YAP dephosphorylation as shown by western blot (**a**, lower arrow), and nuclear translocation as shown by immunofluorescence staining (**b**). (**c**,**d**) Stress-induced TEAD and YAP cytoplasmic translocation is p38-dependent, but Hippo-independent. YAP is constitutively dephosphorylated in Lats KO cells as indicated by YAP phos-tag gel (**c**). Immunofluorescence shows that stress induces YAP and TEAD cytoplasmic translocation in the Lats KO cells, which is blocked by SB203580 treatment (**d**). (**e**) Quantification of *CTGF* mRNA by qRT-PCR in WT and Lats KO cells stimulated with osmotic stress with or without SB203580 treatment. Data are presented as mean ± s.e.m. from $n=3$ independent experiments. (**f**,**g**) Detection of YAP/TAZ localization by immunofluorescence staining in TEAD KO cells stimulated with LPA or serum. Western blotting indicates that YAP dephosphorylation by LPA or serum stimulation is intact in TEAD KO cells (**f**), whereas immunofluorescence shows YAP nuclear accumulation is impaired (**g**). Scale bars in **b**, **d** and **g** are 20 μm. Statistics source data are shown in Supplementary Table 1. Unprocessed original scans of blots are shown in Supplementary Fig. 5.

that YAP-driven cancer cells are highly susceptible to stress-induced TEAD inhibition. To further elucidate the role of TEAD inhibition on YAP-driven cancers, MSTO-211H cells were used as an isogenic model. Growth inhibitory effects resulting from stable expression of p38 were rescued by expression of constitutively active TEAD *in vitro* and *in vivo* (Fig. 4j–m and Supplementary Fig. 4j). Under physiological osmotic stress, TEAD was cytoplasmic in tubule cells of normal kidney tissue, but was nuclear in malignant renal clear cell carcinoma as well as other normal tissues not exposed to osmotic stress (Supplementary Fig. 4k–m). Taken together, our results suggest that regulation of TEAD is important for modulating cancer growth and indicate TEAD as a potential therapeutic target.

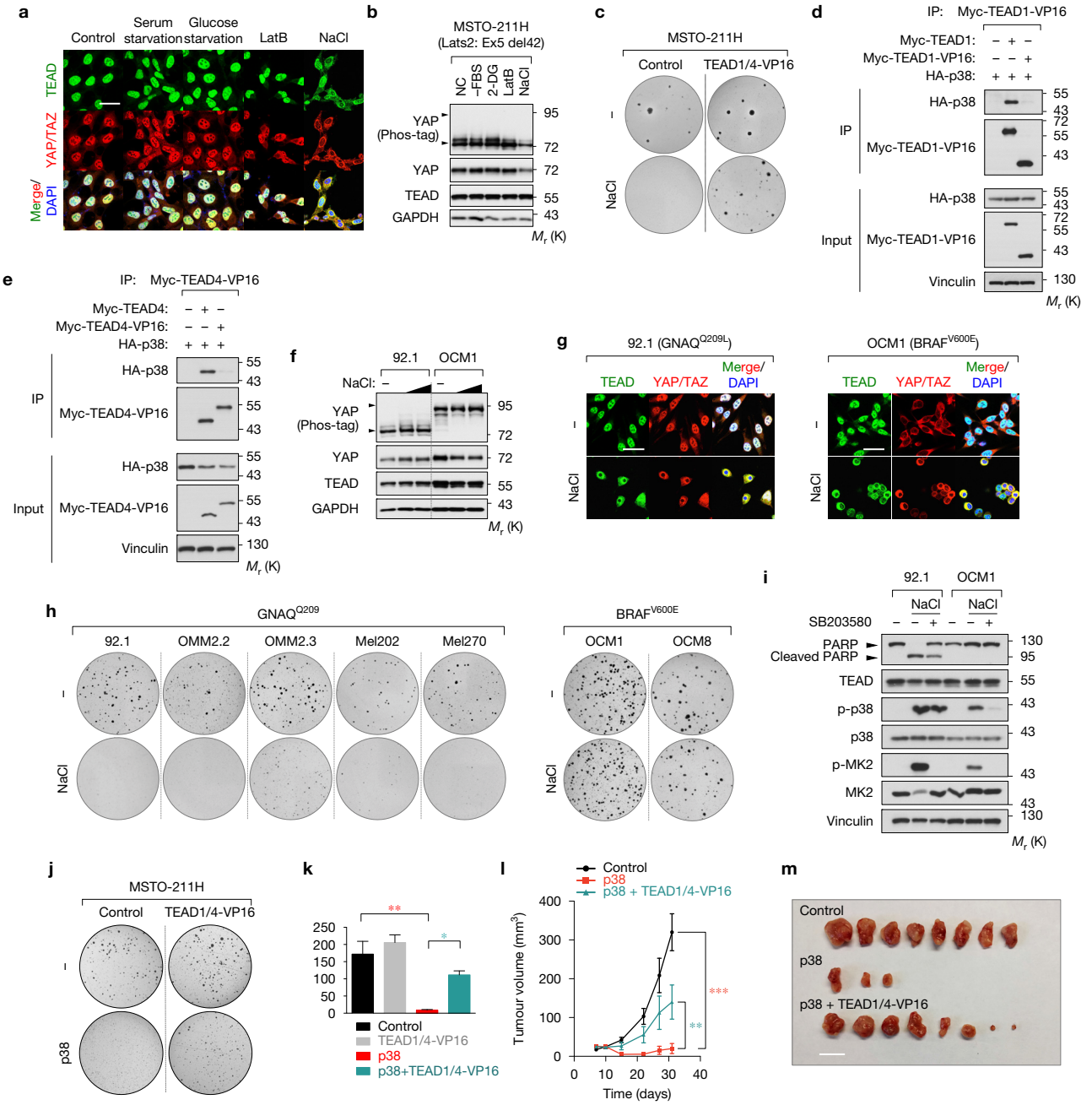

Figure 4 TEAD inhibition restricts YAP-driven cancer cell growth. (**a**,**b**) Effect of osmotic stress on TEAD and YAP cytoplasmic sequestration in MSTO-211H mesothelioma cells. Note that unlike HEK293A (Fig. 1a), serum starvation, glucose starvation and latrunculin B did not induce YAP cytoplasmic localization because of Lats2 mutation in MSTO-211H cells. Only NaCl treatment elicited TEAD and YAP cytoplasmic translocation as detected by immunofluorescence (**a**) despite constitutive YAP dephosphorylation as detected by western blot (**b**). (**c**) Stress-induced TEAD inhibition suppresses anchorage-independent growth. Osmotic stress inhibited colony formation in control, but not TEAD1/4-VP16-expressing MSTO-211H cells. (**d**,**e**) Immunoprecipitation shows that p38 cannot bind TEAD1-VP16 (**d**) or TEAD4-VP16 (**e**). (**f**) Western blotting of YAP phosphorylation status in the UM cell lines 92.1 and OCM1. (**g**) Immunostaining of TEAD and YAP/TAZ in the UM cell lines 92.1 and OCM1 following osmotic stress. Note that YAP displays cytoplasmic staining under normal conditions in OCM1 cells. Scale bars in **a** and **g** are 20 μm. (**h**) Differential effect of TEAD inhibition on anchorage-independent growth of GNAQ-mutant and BRAF-mutant UM cells. Stress-induced TEAD inhibition ablated colony formation in all GNAQ-mutant cell lines, whereas BRAF-mutant cell growth was insensitive. (**i**) Western blot for PARP cleavage in 92.1 and OCM1 cells. NaCl stimulation induces apoptosis in 92.1 but not OCM1 cells. Pretreatment with p38 inhibitor rescues cells from osmotic-stress-induced apoptosis. (**j**) TEAD1/4-VP16 rescues p38-induced inhibition of colony formation of MSTO-211H cells. (**k**) Quantification of **j**. $n=3$ biological replicates. Data are presented as mean ± s.e.m. $^{*}P<0.05$; $^{**}P<0.01$; P values were determined using one-way ANOVA followed by Tukey's multiple comparison test. (**l**) TEAD1/4-VP16 rescues p38-induced inhibition of MSTO-211H *in vivo* tumour xenograft growth. Nude mice were injected with control, p38– or p38+TEAD1/4-VP16-expressing MSTO-211H cells and tumour growth was measured at the indicated times. Data are presented as mean ± s.e.m. $n=4$ mice per group. $^{**}P<0.01$; $^{***}P<0.001$; P values were determined using two-way ANOVA. (**m**) Nude mice were injected with control, p38– or p38+ TEAD1/4-VP16-expressing MSTO-211H cells and tumours were harvested after 4 weeks. Only three tumours developed, out of eight injections, in the p38 group. Scale bar, 10 mm. Unprocessed original scans of blots are shown in Supplementary Fig. 5.

In the present study, we report that the Hippo pathway transcription factor TEAD is regulated through nucleocytoplasmic shuttling. TEAD is regulated by different upstream signals with distinct mechanisms as compared with YAP/TAZ. Many signals, such as serum and energy status, which modulate the localization of YAP, have no effect on TEAD localization. We identified certain environmental stresses that can induce cytoplasmic TEAD translocation. In the case of osmotic stress, TEAD cytoplasmic translocation is mediated by p38 MAPK and independent of the Hippo core kinases. It should be noted that osmotic stress initially induces acute nuclear accumulation of YAP[19,20], then at later stages, induces cytoplasmic translocation of TEAD, and consequently YAP, as an adaptive response to stress. Mechanistically, osmotic-stress-induced cytoplasmic TEAD translocation occurs via direct protein–protein interaction with p38, independent of Hippo. Disruption of TEAD–p38 interaction abolishes TEAD cytoplasmic translocation, resulting in nuclear retention of transcriptionally active TEAD. Cytoplasmic localization of TEAD is also observed in different cellular contexts, such as cell density that is p38-independent, as well as developmental contexts[21,22]. Importantly, stress-induced TEAD inhibition predominates YAP-activating signals by preventing YAP nuclear accumulation, regardless of the phosphorylation status of YAP. Thus, inhibition of TEAD presents a Hippo-pathway-independent avenue of regulating YAP activity, thereby providing a mechanism of controlling its functional output without targeting the Hippo core components Mst and Lats. Moreover, stress-induced TEAD nucleocytoplasmic shuttling is intact in cancer cells that harbour mutations in Hippo pathway upstream components and renders YAP-driven cancer cells highly susceptible to stress-induced growth inhibition. Therefore, pharmacological agents that promote TEAD cytoplasmic localization may be a viable therapeutic strategy for treatment of cancers, especially those with high YAP activity. □

METHODS

Methods, including statements of data availability and any associated accession codes and references, are available in the online version of this paper.

Note: Supplementary Information is available in the online version of the paper

ACKNOWLEDGEMENTS

This work was supported by grants from the National Institutes of Health (CA196878, DE15964 and GM51586) to K.-L.G., the National Research Foundation of Korea (NRF) grant funded by the Korea government (MSIP) (2014R1A5A2009936) to H.-S.J. and by a grant of the Korea Health Technology R&D Project through the Korea Health Industry Development Institute (KHIDI), funded by the Ministry of Health & Welfare, Republic of Korea (grant number: HI17C1560), and the National Research Foundation of Korea (NRF) grant funded by the Korea government (MOE) (2017R1D1A1B03034797) and (MSIP) (2017R1A4A1015328) to H.W.P. K.C.L. and S.W.P. were supported in part by the University of California, San Diego (UCSD) Graduate Training Program in Cellular and Molecular Pharmacology (T32 GM007752).

AUTHOR CONTRIBUTIONS

K.C.L. and H.W.P. designed experiments, performed research, analysed data and wrote the manuscript. T.M., Z.M., H.-S.J. and S.W.P. designed experiments, performed research, analysed data and reviewed the manuscript. Y.S. and J.H. provided reagents and reviewed the manuscript. K.-L.G. designed experiments, analysed data and wrote the manuscript.

COMPETING FINANCIAL INTERESTS

K.-L.G. is a co-founder of and has an equity interest in Vivace Therapeutics. The terms of this arrangement have been reviewed and approved by the University of California, San Diego in accordance with its conflict of interest policies.

Published online at http://dx.doi.org/10.1038/ncb3581

1. Johnson, R. & Halder, G. The two faces of Hippo: targeting the Hippo pathway for regenerative medicine and cancer treatment. *Nat. Rev. Drug Discov.* **13,** 63–79 (2014).
2. Yu, F. X., Zhao, B. & Guan, K. L. Hippo pathway in organ size control, tissue homeostasis, and cancer. *Cell* **163,** 811–828 (2015).
3. Zhao, B. *et al.* TEAD mediates YAP-dependent gene induction and growth control. *Genes Dev.* **22,** 1962–1971 (2008).
4. Yu, F. X. *et al.* Regulation of the Hippo-YAP pathway by G-protein-coupled receptor signaling. *Cell* **150,** 780–791 (2012).
5. Mo, J. S. *et al.* Cellular energy stress induces AMPK-mediated regulation of YAP and the Hippo pathway. *Nat. Cell Biol.* **17,** 500–510 (2015).
6. Wang, W. *et al.* AMPK modulates Hippo pathway activity to regulate energy homeostasis. *Nat. Cell Biol.* **17,** 490–499 (2015).
7. Dupont, S. *et al.* Role of YAP/TAZ in mechanotransduction. *Nature* **474,** 179–183 (2011).
8. Zhao, B. *et al.* Cell detachment activates the Hippo pathway via cytoskeleton reorganization to induce anoikis. *Genes Dev.* **26,** 54–68 (2012).
9. Kim, N. G. & Gumbiner, B. M. Adhesion to fibronectin regulates Hippo signaling via the FAK-Src-PI3K pathway. *J. Cell Biol.* **210,** 503–515 (2015).
10. Sorrentino, G. *et al.* Metabolic control of YAP and TAZ by the mevalonate pathway. *Nat. Cell Biol.* **16,** 357–366 (2014).
11. de Nadal, E., Ammerer, G. & Posas, F. Controlling gene expression in response to stress. *Nat. Rev. Genet.* **12,** 833–845 (2011).
12. Cargnello, M. & Roux, P. P. Activation and function of the MAPKs and their substrates, the MAPK-activated protein kinases. *Microbiol. Mol. Biol. Rev.* **75,** 50–83 (2011).
13. Tanoue, T., Adachi, M., Moriguchi, T. & Nishida, E. A conserved docking motif in MAP kinases common to substrates, activators and regulators. *Nat. Cell Biol.* **2,** 110–116 (2000).
14. Tanoue, T., Maeda, R., Adachi, M. & Nishida, E. Identification of a docking groove on ERK and p38 MAP kinases that regulates the specificity of docking interactions. *EMBO J.* **20,** 466–479 (2001).
15. Estrada-Gelonch, A., Aramburu, J. & Lopez-Rodriguez, C. Exclusion of NFAT5 from mitotic chromatin resets its nucleo-cytoplasmic distribution in interphase. *PLoS ONE* **4,** e7036 (2009).
16. Moroishi, T., Hansen, C. G. & Guan, K. L. The emerging roles of YAP and TAZ in cancer. *Nat. Rev. Cancer* **15,** 73–79 (2015).
17. Yu, F. X. *et al.* Mutant Gq/11 promote uveal melanoma tumorigenesis by activating YAP. *Cancer Cell* **25,** 822–830 (2014).
18. Murakami, H. *et al.* LATS2 is a tumor suppressor gene of malignant mesothelioma. *Cancer Res.* **71,** 873–883 (2011).
19. Hong, A. W. *et al.* Osmotic stress-induced phosphorylation by NLK at Ser128 activates YAP. *EMBO Rep.* **18,** 72–86 (2017).
20. Moon, S. *et al.* Phosphorylation by NLK inhibits YAP-14-3-3-interactions and induces its nuclear localization. *EMBO Rep.* **18,** 61–71 (2017).
21. Home, P. *et al.* Altered subcellular localization of transcription factor TEAD4 regulates first mammalian cell lineage commitment. *Proc. Natl Acad. Sci. USA* **109,** 7362–7367 (2012).
22. Cagliero, J., Forget, A., Daldello, E., Silber, J. & Zider, A. The Hippo kinase promotes Scalloped cytoplasmic localization independently of Warts in a CRM1/Exportin1-dependent manner in *Drosophila*. *FASEB J.* **27,** 1330–1341 (2013).

METHODS

Cell culture. All cell lines were maintained at 37 °C with 5% CO_2. HEK293A cells were cultured in DMEM (Invitrogen, 11965118) and uveal melanoma and mesothelioma cell lines were cultured in RPMI (Invitrogen, 11875119) containing 10% FBS (Gibco, 10437028) and 50 μg ml^{-1} penicillin/streptomycin (Invitrogen, 15140122). MCF10A cells were cultured in DMEM-F12 supplemented with 5% horse serum (Invitrogen, 26050088), 20 ng ml^{-1} EGF (Peprotech, AF-100-15), 0.5 μg ml^{-1} hydrocortisone (Sigma, H4001-25G), 100 ng ml^{-1} cholera toxin (Sigma, C8052-2MG) and 10 μg ml^{-1} insulin (Sigma, I1882-100MG). YAP-inhibitory signals and environmental stresses included the following: serum starvation (16 h), glucose starvation (2-DG, 25 mM, 2 h), PKA activation (forskolin, 10 μM, 1 h), disruption of F-actin (latrunculin B, 0.1 μg ml^{-1}, 1 h), Src inhibition (dasatinib, 5 μM, 6 h), inhibition of the mevalonate synthesis (cerivastatin, 2 μM, 6 h), NaCl (200 mM, 6 h), sorbitol (0.5 M, 6 h), high cell density (2 day post-confluent) and cell detachment (1 h). No cell lines used in this study were found in the database of commonly misidentified cell lines that is maintained by ICLAC and NCBI Biosample. The cell lines were not authenticated. Cells lines were tested and confirmed to be free of mycoplasma.

Induction of osmotic stress and p38 inhibitor treatment. Cells were treated with either 200 mM NaCl or 0.5 M sorbitol for 6 h. The p38 inhibitors SB203580 (S1076) (40 μM) and PH797840 (S2726) (30 μM) were purchased from Selleckchem and cells were treated 2 h prior to osmotic stress exposure.

Transfection and viral infection. Cells were transfected with plasmid DNA using PolyJet Reagent (Signagen Laboratories) according to the manufacturer's protocol. Cells were transfected with (pCDNA3) Flag-p38 or (pCDNA3) HA-p38, (pCDNA3) Flag-MKK3 and (pRK5) Myc-TEAD4.

92.1, OCM1 and MSTO-211H cells stably expressing empty vector; p38 and MKK3; and p38, MKK3 and TEAD1/4-VP16 were generated by retroviral and lentiviral infection. HEK293T packaging cells were transfected with empty vector, (pHIV puro) p38, (pQCXIH) MKK3 and (pHIV GFP) TEAD1/4-VP16 constructs. At 48 h after transfection, retroviral and lentiviral supernatant was filtered through a 0.45 μm filter, supplemented with 8 μg ml^{-1} Polybrene, and used for infection. At 48 h after infection, cells were selected with puromycin (1 μg ml^{-1}) and hygromycin (200 μg ml^{-1}) and FACS sorted for GFP expression.

Animal work. NU/J (nude mice) were purchased from Jackson Laboratory (Bar Harbor). For tumour xenograft models, MSTO-211H cells (5×10^6) were injected subcutaneously into both flanks of 8–12-week-old female nude mice. Four mice were assigned to each group. The investigators were not blinded to allocation during experiments and outcome assessment. Tumour height and width were measured with a calliper every 2–3 days to calculate tumour volume ($= \text{width}^2 \times \text{height} \times 0.523$). Mice were euthanized 4 weeks post engraftment. All animal experiments were approved by the University of California, San Diego, Institutional Animal Care and Use Committee.

Antibodies. The following antibodies were purchased from Cell Signaling and used at the indicated dilution for western blot analysis, immunohistochemistry and immunofluorescence: pan-TEAD (13295, 1:1,000), p38 MAPK (8690, 1:1,000), phospho-p38 MAPK (4511, 1:1,000), YAP (14074, 1:1,000), TAZ (4883, 1:1,000), Lats1 (3477, 1:1,000), p-MK2 (3007, 1:1,000), p-ERK (4370, 1:1,000), DYKDDDDK tag (2368, 1:1,000), Myc tag (2276, 1:1,000), p38α (2371, 1:1,000), p38β (2339, 1:1,000), p38γ (2307, 1:1,000) and p38δ (2308, 1:1,000). The following antibodies were purchased from Santa Cruz Biotechnology and used at the indicated dilution for western blot analysis and immunofluorescence: YAP (sc-101199, 1:1,000), HA (sc-7392, 1:5,000), Myc (sc-40, 1:5,000), GAPDH (sc-25778, 1:1,000). TEAD4 (ab58310, 1:1,000) was purchased from Abcam, Flag (A8592, 1:10,000) and vinculin (V9131, 1:5,000) were purchased from Sigma, TEAD1 (610923, 1:1,000) was purchased from BD Biosciences, Lats2 (A300-479A, 1:1,000) was purchased from Bethyl Laboratories, and NFAT5 (bs-9473R OWL 1:1,000) was purchased from One World Lab.

Generation of knockout cells and mutagenesis. pSpCas9(BB)-2A-Puro (PX459) was a gift from F. Zhang (Broad Institute of MIT and Harvard, USA) (Addgene plasmid no. 48139; ref. 23). The nucleotide guide sequences were designed using the CRISPR design tool at http://crispr.mit.edu. Single-guide RNAs (sgRNAs) were cloned into the PX459 expression vector. HEK293A cells were transfected using PolyJet DNA *in vitro* Transfection Reagent according to the manufacturer's instructions. At 24 h post transfection, cells were selected with puromycin for 2–3 days. Following removal of puromycin, cells were allowed to recover in regular growth media for 24 h before being single-cell-sorted by FACs (UCSD; Human Embryonic Stem Cell Core, BDInflux) into a 96-well-plate format. Single clones were expanded and screened by protein immunoblotting, genomic sequencing and functional assays. Lats KO, Mst KO and MAP4K KO cells were generated as previously described[24,25].

Guide sequences: p38α: 5′-3′ AGCTCCTGCCGGTAGAACGT; p38β: 5′-3′ CCA CGCGCGCAGAACGTACC; p38γ: 5′-3′ GGACGGCCGCACCGGCGCTA; p38δ: 5′-3′ TCCCCGACGCACGTCGGCAG; TEAD1: 5′-3′ TGGCAGTGGCCGAGACG ATC; TEAD2: 5′-3′ AGATAGGTGGGACGCCGGCG; TEAD4: 5′-3′ CTCAAGGA TCTCTTCGAACG.

p38 and TEAD site-directed mutagenesis was carried out using Q5 Hot Start High Fidelity DNA Polymerase from New England Biolabs (M0494) per the manufacturer's protocol.

RNA extraction, cDNA synthesis and quantitative real-time PCR analysis. Cells were harvested for RNA extraction using the RNeasy Plus mini kit (QIAGEN, 74136). RNA samples were reverse-transcribed to complementary DNA (cDNA) using iScript reverse transcriptase (Bio-Rad, 1708891). qRT-PCR was performed using the KAPA SYBR FAST qPCR kit (Kapa Biosystems, KK4605) and the 7300 real-time PCR system (Applied Biosystems).

Primer sequences used were as previously described[4,24].

Immunofluorescent microscopy. Cells were seeded in 12-well plates on coverslips 2 days prior to experimentation. Coverslips were pretreated with poly-L-ornithine solution (Sigma, P4957) diluted 1:20 at 37 °C for 15 min with a quick phosphate-buffered saline (PBS) wash prior to cell seeding. Cells were fixed in 4% paraformaldehyde (Electron Microscopy Sciences, 2280) for 15 min followed by permeabilization with 0.1% Triton-X for 5 min. Cells were blocked in 3% BSA for 1 h and incubated overnight at 4 °C in primary antibodies diluted in 3% BSA. Secondary antibodies were diluted in 3% BSA and incubated for 1 h. Slides were mounted with Prolong gold antifade reagent with DAPI (Invitrogen, P36931). Each image is a single *Z* section at the same cellular level. Images were captured with a Nikon Eclipse T*i* confocal microscope. Images depicted in figures were exported from NIS elements imaging software.

Immunohistochemistry. Kidney tissue arrays were purchased from US Biomax. Tissues were subject to heat-induced antigen retrieval using 10 mM sodium citrate buffer followed by 3% H_2O_2 for 30 min to quench endogenous peroxidase activity. Sections were incubated overnight at 4 °C with pan-TEAD antibody and detected using Vectastain elite ABC kit and DAB Peroxidase Substrate kit (Vector Laboratories) as per the manufacturer's protocol.

Western blot and immunoprecipitation. Immunoblotting was performed using a standard protocol. Phos-tag reagents were purchased from Wako Chemicals, and gels containing phos-tag were prepared according to the manufacturer's instructions. For immunoprecipitations, cells were rinsed twice with ice-cold PBS and lysed in ice-cold lysis buffer (0.15 M NaCl, 0.05 M Tris-HCl, 0.5% Triton X-100, and one tablet each of EDTA-free protease inhibitors (Roche, 11873580001) and phosphatase inhibitor (Thermo Fisher, 88667) per 50 ml). For immunoprecipitations, primary antibodies were added to the lysates and incubated with rotation overnight at 4 °C. Ten microlitres of magnetic protein A/G beads (Thermo Fisher, 88802) were added and incubated for an additional 2 h. Immunoprecipitates were washed three times with lysis buffer. Immunoprecipitated proteins were denatured by the addition of sample buffer and boiling for 5 min, resolved by 9% SDS–PAGE, and analysed via western blot analysis.

***In vitro* kinase assay.** To analyse p38 kinase activity, HEK293A cells were transfected with WT or kinase mutant p38α. p38γ and p38δ were purchased from SignalChem. Cells were collected and p38 was immunoprecipitated as described above. Immunoprecipitates were washed with kinase assay buffer (25 mM HEPES pH 7.4, 25 mM $MgCl_2$ and 2 mM dithiothreitol) and subjected to a kinase assay in kinase assay buffer along with 500 μM AT-γ-S. GST-ATF2, GST-TEAD4 or GST-TEAD4-4SP fusion proteins were used as substrates. Reactions were incubated for 30 min at 30 °C. p-Nitrobenzyl mesylate (Sigma, A1388) was added to the kinase reactions and incubated for 1 h to alkylate the thiophosphorylation sites on the substrates. Reactions were terminated with sample buffer and resolved on 9% SDS–PAGE. A thiophosphate ester antibody (Abcam, ab92570) was used to detect substrate phosphorylation.

Soft agar colony growth. Each 6-well plate was coated with 1.5 ml of bottom agar (DMEM containing 10% FBS and 0.5% Difco agar noble). Various cells (5×10^3) were suspended in 1.5 ml of top agar (DMEM containing 10% FBS and 0.35% Difco agar noble) into each well. Cells were incubated for approximately three weeks and

DOI: 10.1038/ncb3581

replaced with fresh medium containing 50 mM NaCl every three days. Colonies were stained using 0.005% crystal violet.

Statistics and reproducibility. The experiments for Fig. 4l,m and Supplementary Fig. 4l,m were completed once. The experiments shown in Figs 2b,f and 4j, and Supplementary Figs 1h, 2b–d, 3f and 4h–j,l–m are representative of 2 independent experiments performed with similar results. All other experiments are representative of at least 3 independent repeats. Data are presented as mean ± s.e.m. *P* values were determined using one-way ANOVA followed by Tukey's multiple comparison test or two-way ANOVA as noted in the figure legends.

Data availability. Source data for Figs 1g,h and 3e and Supplementary Figs 1j and 4j have been provided as Supplementary Table 1. All other data supporting the findings of this study are available from the corresponding author on reasonable request.

23. Ran, F. A. *et al.* Genome engineering using the CRISPR-Cas9 system. *Nat. Protoc.* **8,** 2281–2308 (2013).
24. Park, H. W. *et al.* Alternative Wnt signaling activates YAP/TAZ. *Cell* **162,** 780–794 (2015).
25. Meng, Z. *et al.* MAP4K family kinases act in parallel to MST1/2 to activate LATS1/2 in the Hippo pathway. *Nat. Commun.* **6,** 8357 (2015).

nature cell biology

DOI: 10.1038/ncb3581

In the format provided by the authors and unedited.

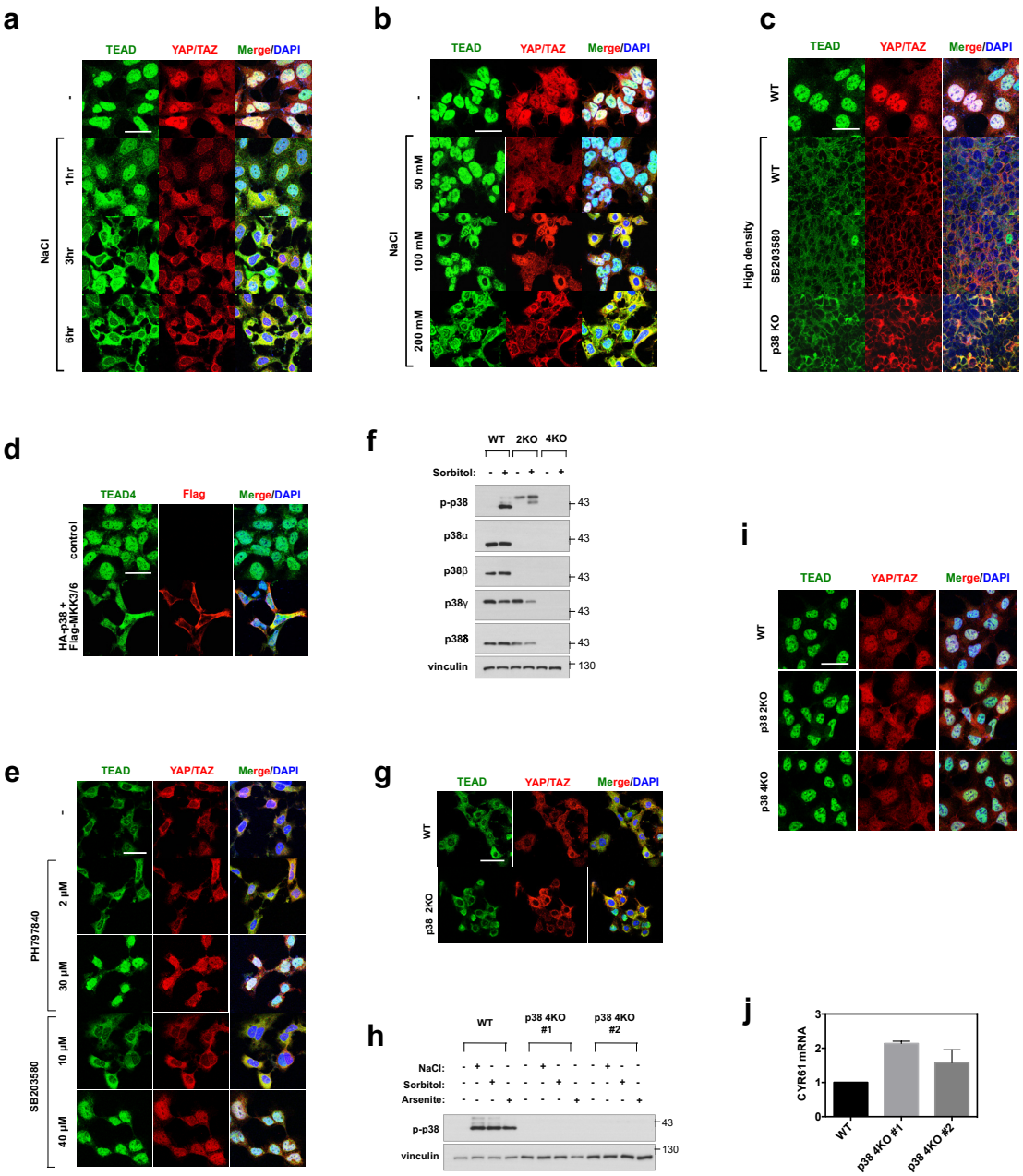

Supplementary Figure 1 Osmotic stress induces TEAD cytoplasmic translocation. **a,** Time course of osmotic stress-induced TEAD cytoplasmic translocation. HEK293A cells were treated with NaCl for 0, 1, 3, or 6 hours and stained for immunofluorescence. **b,** Dose response for NaCl-induced TEAD cytoplasmic translocation. HEK293A cells were stimulated with different concentrations of NaCl for 6 hr and stained for immunofluorescence. TEAD cytoplasmic translocation occurs from100mM NaCl. **c,** High cell density-induced TEAD cytoplasmic localization is p38 independent. Immunofluorescence shows inhibition or KO of p38 upon high cell density has no effect on TEAD cytoplasmic translocation. **d,** Cells ectopically expressing MKK3/p38 were stained for immunofluorescence. MKK3/p38 promotes TEAD4 cytoplasmic translocation. **e,** Dose response for p38 inhibitor treatment. HEK293A cells were pre-treated with different doses of p38 inhibitors as indicated, followed by NaCl stimulation and stained for immunofluorescence. **f,** Western blot of p38α/β knockout cells show upregulation of p38δ/γ isoforms. **g,** p38 2KO cells were stained for immunofluorescence. Deletion of p38α/β isoforms is not sufficient to inhibit TEAD cytoplasmic translocation. **h,** Immunoblotting for p-p38 in p38 4KO cells shows impaired p38 activity under various p38 activating stimuli (200 mM NaCl, 500 μM sorbitol, 500 μM arsenite). **i,j** p38 4KO shows no effect on TEAD localization (i) or target gene expression, as measured by qRT-PCR (j) under basal conditions. Scale bars in a-e, g, and i are 20μm. Data are presented as mean ± s.e.m. from *n=3* independent experiments. Statistics source data are shown in Supplementary Table 1. Unprocessed scans of blots are shown in Supplementary Figure 5.

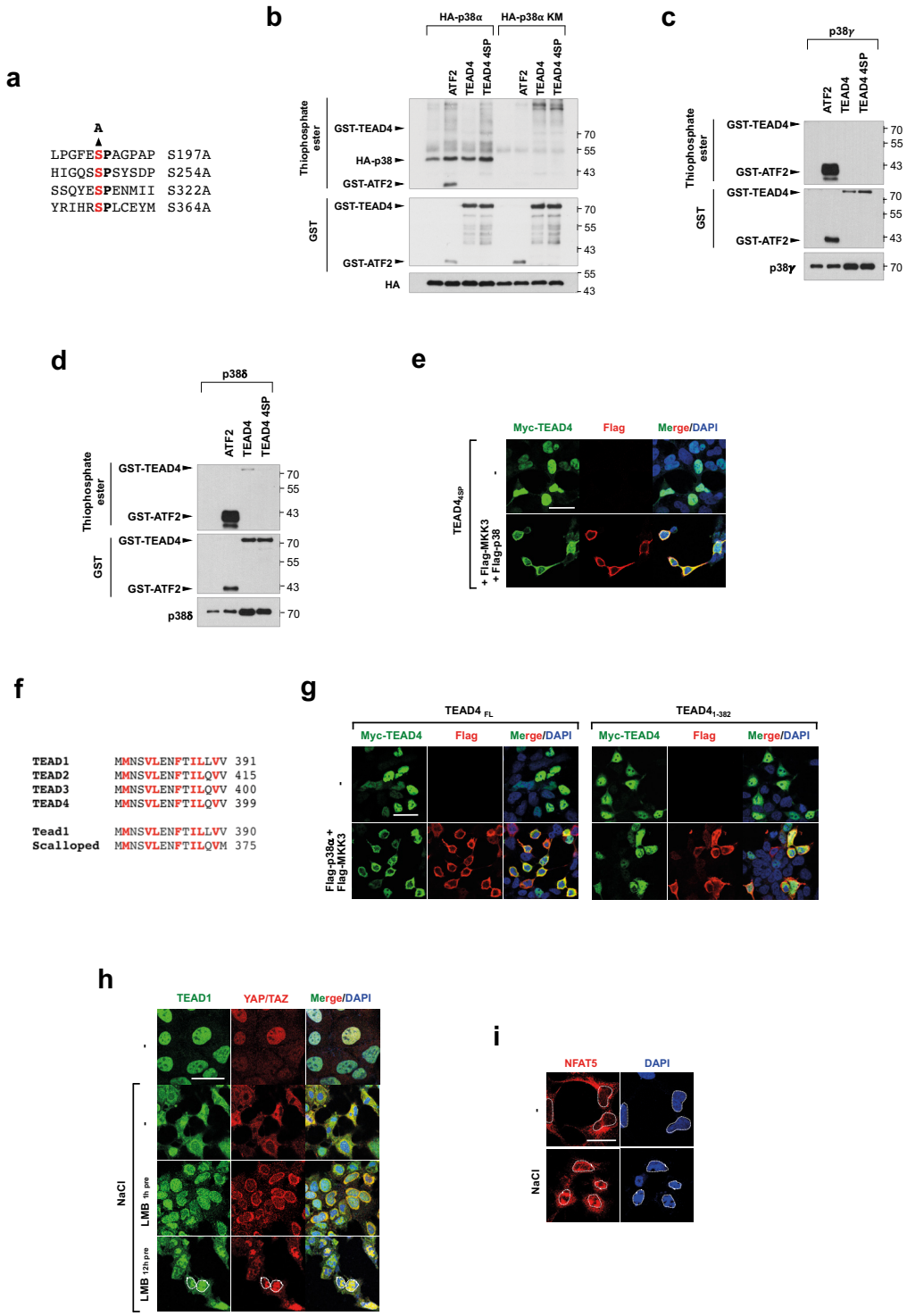

Supplementary Figure 2 Phosphorylation of TEAD by p38 is not required for cytoplasmic translocation. **a,** Sequence of TEAD4-4SP construct harboring mutations in putative p38 phosphorylation sites. **b-d,** TEAD is a poor substrate for p38 phosphorylation. *In vitro* kinase assay for p38α (b), p38γ (c), and p38δ (d) using TEAD as a substrate. No phosphorylation or weak phosphorylation was detected in TEAD4 WT, which was further ablated in TEAD4-4SP, whereas ATF2 was effectively phosphorylated by p38. **e,** Detection of TEAD4-4SP cytoplasmic translocation by p38 using immunofluorescence. **f,** Sequence of putative TEAD nuclear export signal. **g,** TEAD cytoplasmic translocation requires a nuclear export signal. Immunofluorescence shows truncation of TEAD disrupting a putative nuclear export signal in TEAD (1-382) mutant inhibits CRM1-dependent TEAD nuclear export compared to full length TEAD. **h,** TEAD cytoplasmic translocation is a CRM1-dependent process. HEK293A cells were pretreated with LMB for the indicated times followed by NaCl stimulation and staining for immunofluorescence. Pretreatment with LMB inhibits TEAD cytoplasmic translocation. **i,** Immunofluorescence of NFAT5 nuclear translocation upon NaCl stimulation. Scale bars in e and g-i are 20μm. Unprocessed scans of blots are shown in Supplementary Figure 5.

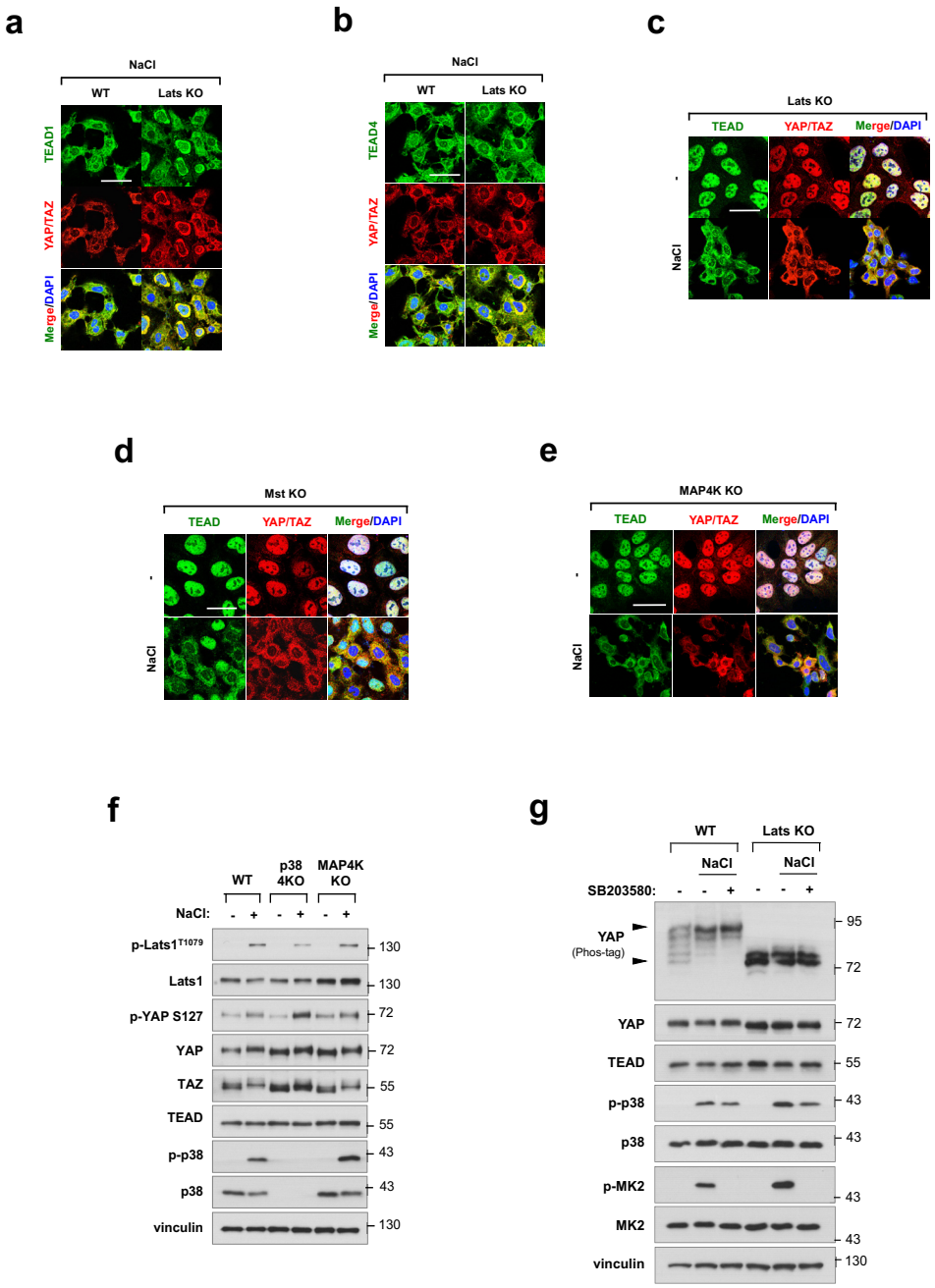

Supplementary Figure 3 Stress-induced TEAD cytoplasmic translocation is independent of Hippo pathway. **a, b,** Stress-induced TEAD cytoplasmic translocation is independent of Lats1/2. WT and Lats KO cells were stimulated with NaCl and stained with anti-TEAD1 (a) or anti-TEAD4 (b) antibody for immunofluorescence. **c, d, e,** Stress-induced TEAD cytoplasmic translocation is independent of Hippo core kinases and MAP4K. Lats KO (c), Mst KO (d), and MAP4K KO (e) cells were treated with NaCl and stained for immunofluorescence. **f,** Western blot showing MAP4K and p38 are independent branches of the MAPK pathway. **g,** Western blot showing stress-activated p38 does not affect YAP phosphorylation status. Scale bars in a-e are 20μm. Unprocessed scans of blots are shown in Supplementary Figure 5.

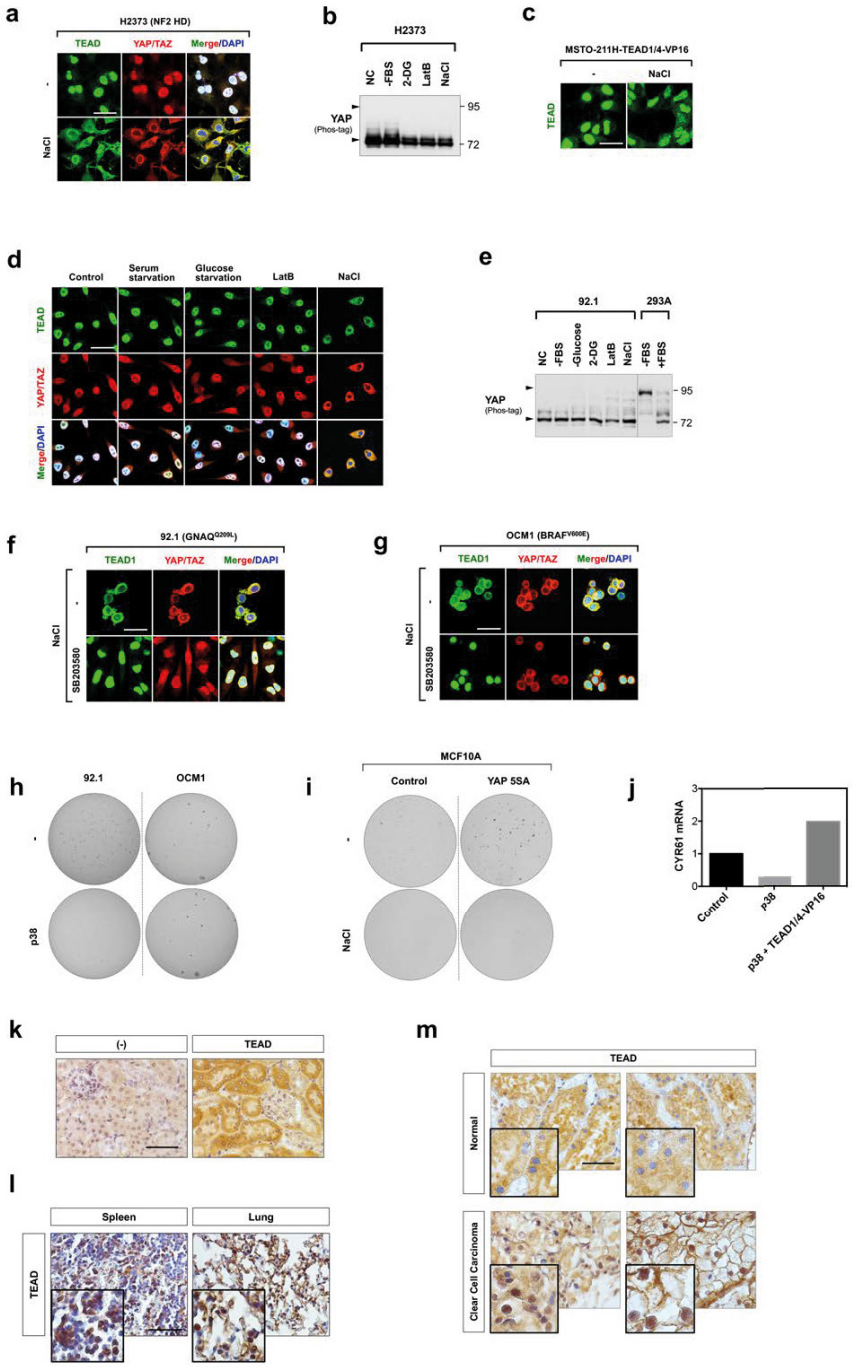

Supplementary Figure 4 Stress-induced TEAD inhibition uncouples YAP localization and dephosphorylation in YAP-driven cancer cells. **a, b,** Stress-induced TEAD and YAP/TAZ cytoplasmic translocation in H2373 mesothelioma cells, which have homozygous deletion of NF2. Immunofluorescence showing NaCl stimulation induces TEAD and subsequent YAP/TAZ cytoplasmic sequestration (a), despite constitutive dephosphorylation of YAP as shown by western blot (b). NC, normal condition. **c,** Nuclear localization of TEAD-VP16 in the presence of osmotic stress. MSTO-211H cells stably expressing TEAD1/4-VP16 construct were treated with NaCl and stained for immunofluorescence. **d, e,** Stress promotes TEAD and YAP cytoplasmic sequestration in YAP-driven uveal melanoma cells. 92.1 cells were treated with YAP-inhibiting stimuli as in Fig. 1a, b. NaCl treatment elicits TEAD and YAP cytoplasmic translocation shown by immunofluorescence (d), despite constitutive dephosphorylation of YAP shown by western blot (e). **f, g,** p38 mediates stress-induced TEAD cytoplasmic translocation in UM cell lines. Immunofluorescence shows treatment with SB203580 blocks NaCl-induced cytoplasmic translocation of TEAD in 92.1 (f) and OCM1 (g). **h,** p38 expression inhibits colony formation of GNAQ-mutant 92.1 cells but not BRAF-mutant OCM1 cells. **i,** Colony growth assay showing osmotic stress inhibits anchorage independent growth of YAP-5SA transformed MCF10A. **j,** Expression of p38 reduces target gene expression induced by hyperactive YAP as measured by qRT-PCR. Target gene expression is rescued by constitutively active TEAD. Data are presented as mean from *n=2* independent experiments. **k-m,** Immunohistochemistry staining of TEAD. Negative control staining for pan-TEAD antibody (left) and normal kidney tissue staining with pan-TEAD (right) (k). Nuclear staining of TEAD detected in mouse spleen and lung tissues (l). Cytoplasmic staining of TEAD is detected in tubule cells of normal kidney while nuclear staining is detected in renal clear cell carcinomas derived from transformed tubule cells (m). Scale bars in a, c-d, and f-g are 20μm. Scale bars in k-m are 50 μm. Statistics source data are shown in Supplementary Table 1. Unprocessed scans of blots are shown in Supplementary Figure 5.

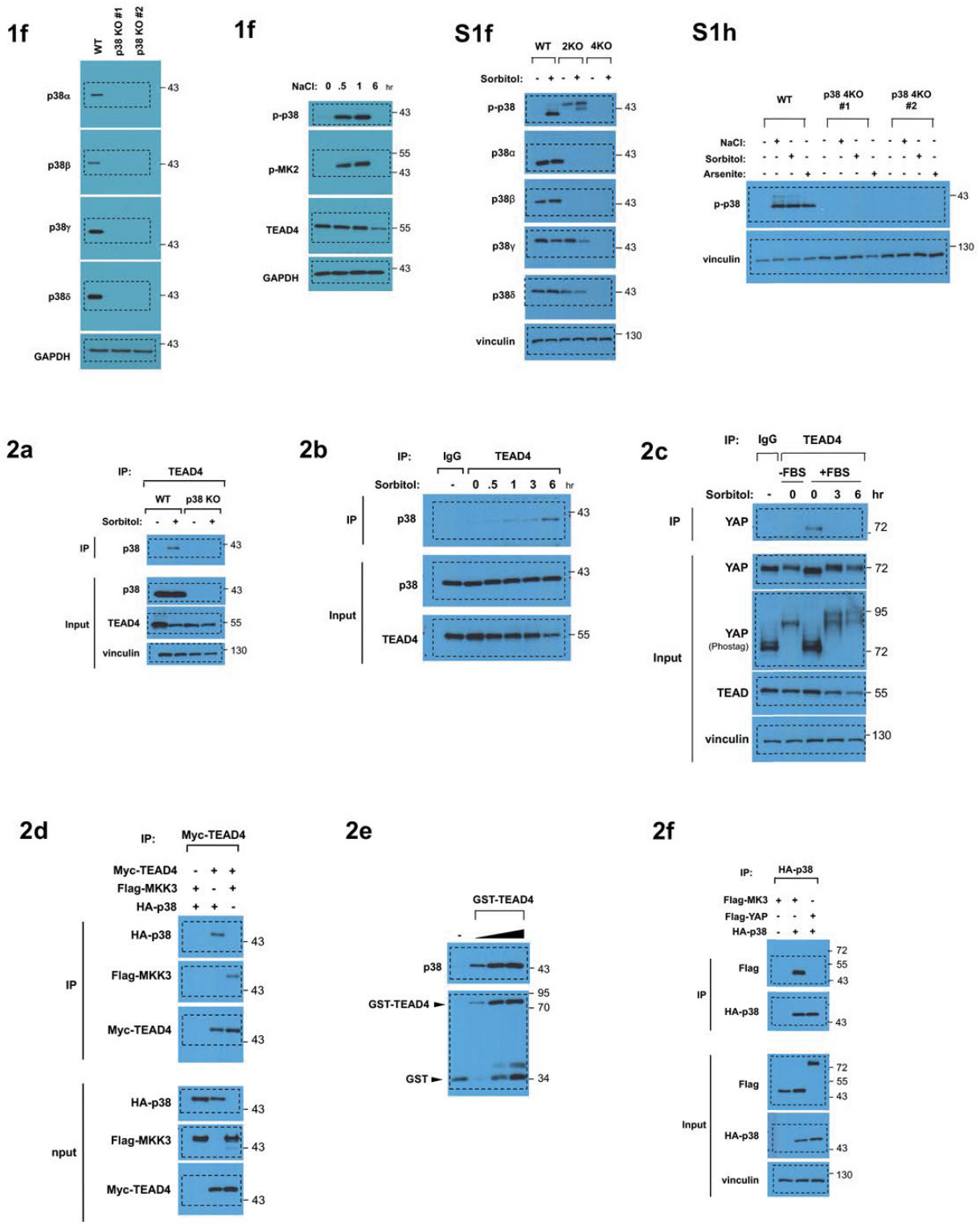

Supplementary Figure 5 Unprocessed scans of western blots.

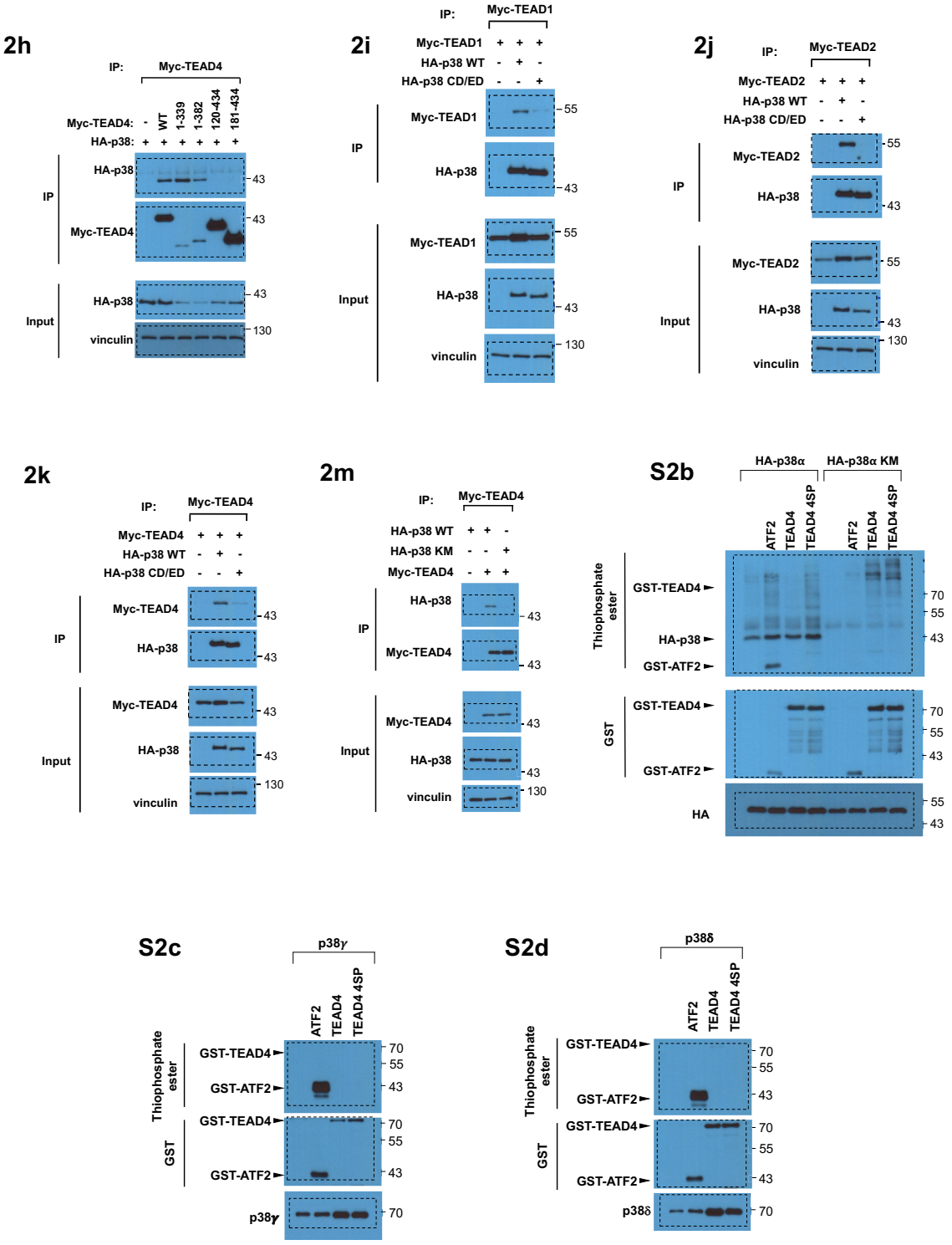

Supplementary Figure 5 Continued

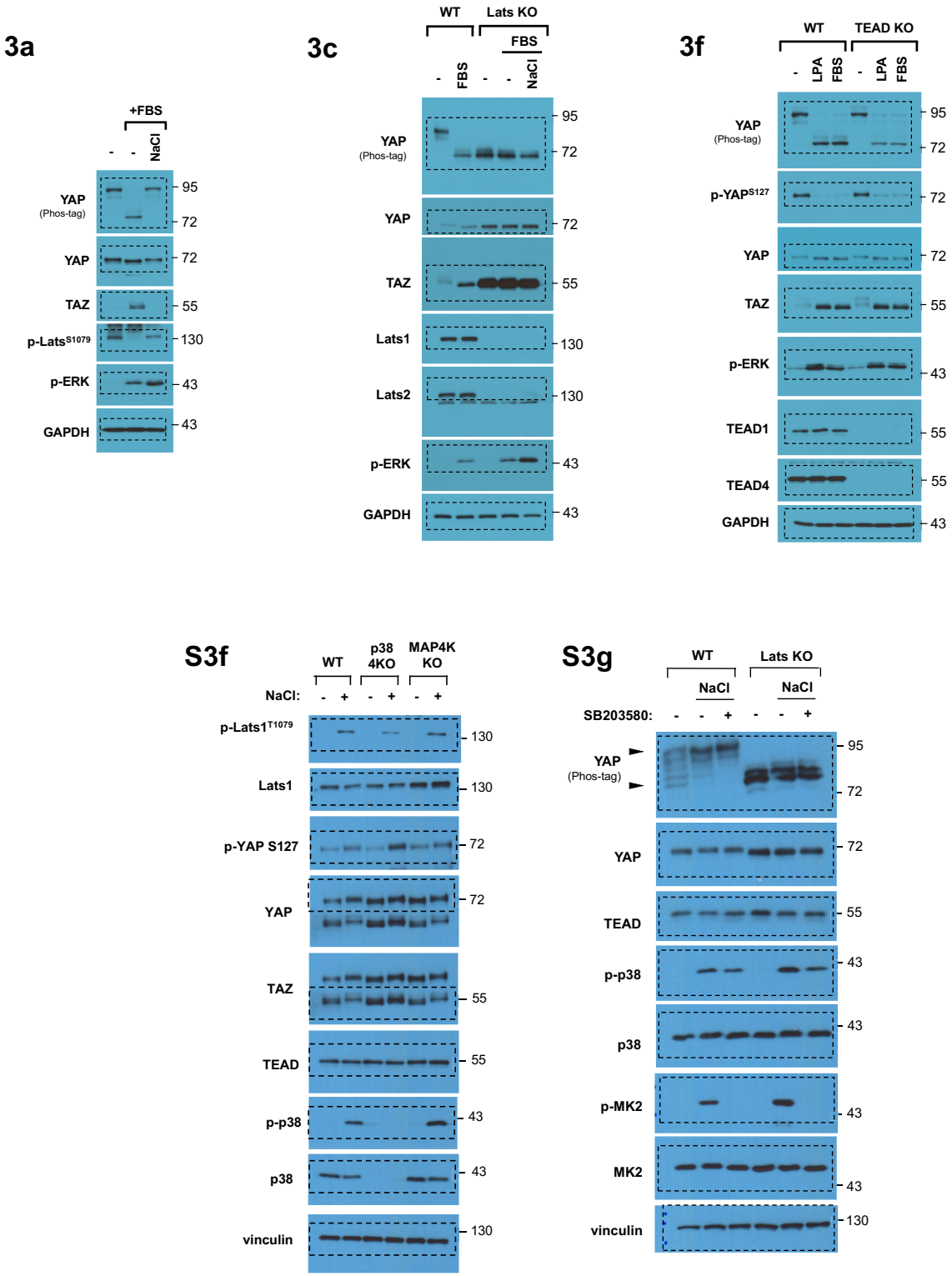

Supplementary Figure 5 Continued

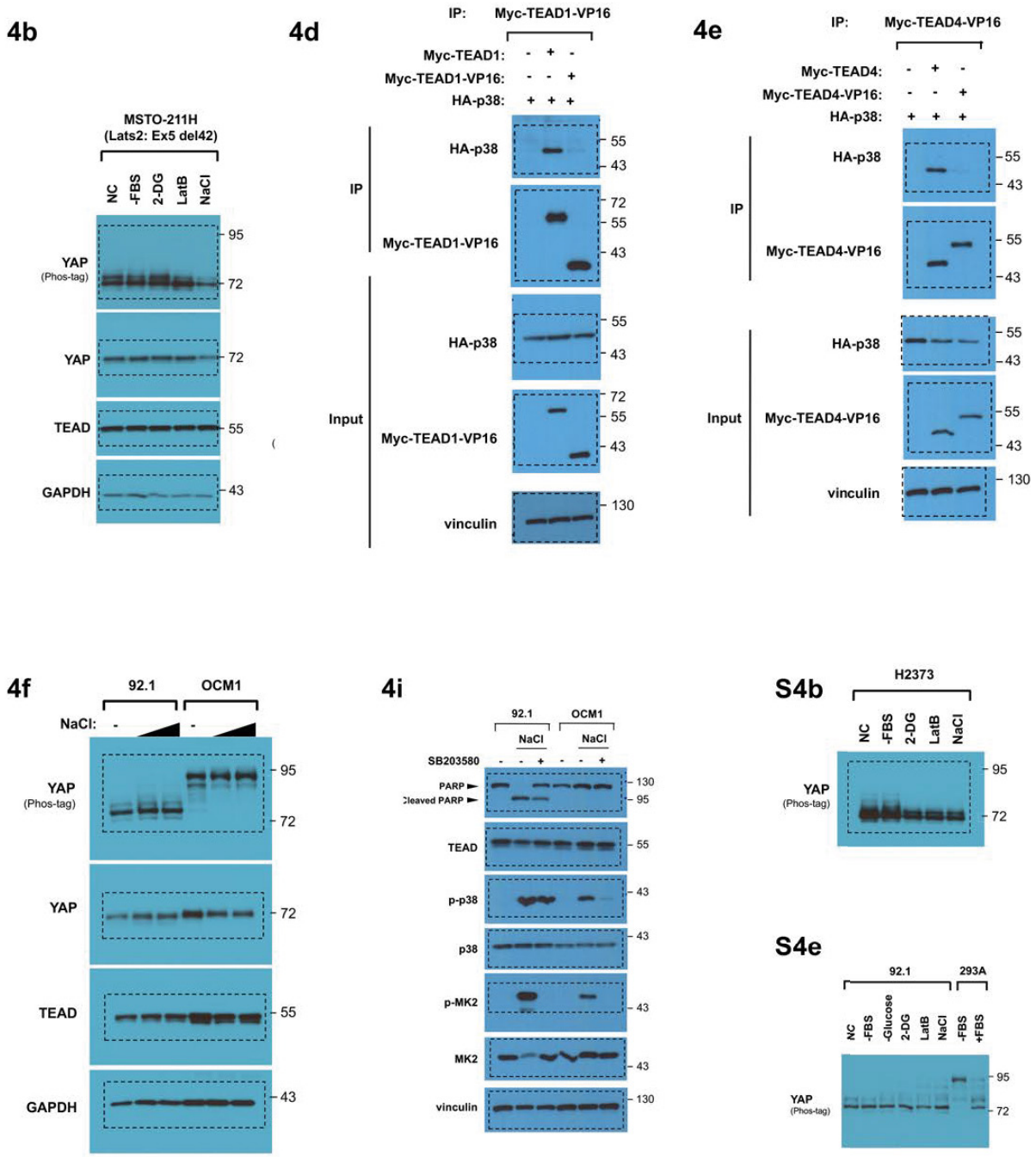

Supplementary Figure 5 Continued

Supplementary Table Legends

Supplementary Table 1 Statistics source data.

nature research

Corresponding Author: Kun-Liang Guan

Date: Jun 6, 2017

Life Sciences Reporting Summary

Nature Research wishes to improve the reproducibility of the work we publish. This form is published with all life science papers and is intended to promote consistency and transparency in reporting. All life sciences submissions use this form; while some list items might not apply to an individual manuscript, all fields must be completed for clarity.

For further information on the points included in this form, see Reporting Life Sciences Research. For further information on Nature Research policies, including our data availability policy, see Authors & Referees and the Editorial Policy Checklist.

Experimental design

1. Sample size

   Describe how sample size was determined.

   We predicted a 30% reduction in tumor growth and calculated sample size using power analysis (DOI: 10.4103/0976-500X.119726) using an SD of 20 (doi:10.4049/jimmunol.1300448) and d of 30. Calculations were made using a type I error of 5% at 80% power. n=6.97. Allowing for 10% attrition, we used n=8 tumors.

2. Data exclusions

   Describe any data exclusions.

   No data were excluded from these analysis

3. Replication

   Describe whether the experimental findings were reliably reproduced.

   All replication attempts were successful

4. Randomization

   Describe how samples/organisms/participants were allocated into experimental groups.

   8-12 week female nude mice were chosen as xenograft hosts. As the mice age they lose immune deficiency, thus 8-12 week mice are ideal. Female mice were chosen as aggressive behavior among male mice may affect measurements of tumor growth. Mice were randomly allocated into experimental groups.

5. Blinding

   Describe whether the investigators were blinded to group allocation during data collection and/or analysis.

   No blinding was carried out.

   Note: all studies involving animals and/or human research participants must disclose whether blinding and randomization were used.

6. Statistical parameters

   For all figures and tables that use statistical methods, confirm that the following items are present in relevant figure legends (or the Methods section if additional space is needed).

n/a	Confirmed	
☐	☒	The exact sample size (*n*) for each experimental group/condition, given as a discrete number and unit of measurement (animals, litters, cultures, etc.)
☐	☒	A description of how samples were collected, noting whether measurements were taken from distinct samples or whether the same sample was measured repeatedly.
☐	☒	A statement indicating how many times each experiment was replicated
☐	☒	The statistical test(s) used and whether they are one- or two-sided (note: only common tests should be described solely by name; more complex techniques should be described in the Methods section)
☒	☐	A description of any assumptions or corrections, such as an adjustment for multiple comparisons
☐	☒	The test results (e.g. *p* values) given as exact values whenever possible and with confidence intervals noted
☐	☒	A summary of the descriptive statistics, including central tendency (e.g. median, mean) and variation (e.g. standard deviation, interquartile range)
☐	☒	Clearly defined error bars

See the web collection on statistics for biologists for further resources and guidance.

Software

Policy information about availability of computer code

7. Software

Describe the software used to analyze the data in this study.	Prism was used for all statistical analysis

For all studies, we encourage code deposition in a community repository (e.g. GitHub). Authors must make computer code available to editors and reviewers upon request. The *Nature Methods* guidance for providing algorithms and software for publication may be useful for any submission.

Materials and reagents

Policy information about availability of materials

8. Materials availability

Indicate whether there are restrictions on availability of unique materials or if these materials are only available for distribution by a for-profit company.	There are no restrictions for any of the materials

9. Antibodies

Describe the antibodies used and how they were validated for use in the system under study (i.e. assay and species).	The following antibodies were purchased from Cell Signaling and used at the indicated dilution for western blot analysis, immunohistochemistry, and immunofluorescence: pan-TEAD (D3F7L) (13295, 1:1000), p38 MAPK (D13E1) (8690, 1:1000), phospho-p38 MAPK (D3F9) (4511, 1:1000), YAP (D8H1X) (14074, 1:1000), TAZ (4883, 1:1000), Lats1 (C66B5) (3477, 1:1000), p-MK2 (27B7) (3007, 1:1000), p-ERK (D13.14.4E) (4370, 1:1000), DYKDDDDK tag (2368, 1:1000), Myc tag (9B11) (2276, 1:1000), p38a (7D6) (2371, 1:1000), p38b (C28C2) (2339, 1:1000), p38g (2307, 1:1000), and p38d (10A8) (2308, 1:1000). The following antibodies were purchased from Santa Cruz Biotechnology and used at the indicated dilution for western blot analysis and immunofluorescence: YAP (63.7) (sc-101199, 1:1000), HA (F-7) (sc-7392, 1:5000), Myc (9E10) (sc-40, 1:5000), GAPDH (sc-25778, 1:1000). TEAD4 (ab58310, 1:1000) was purchased from Abcam, Flag (M2) (A8592, 1:10,000) and vinculin (hVIN-1) (V9131, 1:5000) was purchased from Sigma, TEAD1 (31) (610923, 1:1000) was purchased from BD Biosciences, Lats2 (A300-479A, 1:1000) was purchased from Bethyl Laboratories, and NFAT5 (bs-9473R OWL 1:1000) was purchased from One World Lab.

10. Eukaryotic cell lines

a. State the source of each eukaryotic cell line used.	Mesothelioma cell lines were obtained from Dr. Yoshitaka Sekido. Uveal melanoma cell lines were a gift from Dr. Martine Jager.
b. Describe the method of cell line authentication used.	Cell lines were not authenticated
c. Report whether the cell lines were tested for mycoplasma contamination.	Cell lines were tested to be free of mycoplasma contamination.
d. If any of the cell lines used in the paper are listed in the database of commonly misidentified cell lines maintained by ICLAC, provide a scientific rationale for their use.	No cells lines listed in the paper are in the database of commonly misidentified cell lines.

Animals and human research participants

Policy information about studies involving animals; when reporting animal research, follow the ARRIVE guidelines

11. Description of research animals

Provide details on animals and/or animal-derived materials used in the study.

NU/J (nude mice) were purchased from Jackson Laboratory (Bar Harbor, ME, USA). For tumor xenograft models, MSTO-211H cells (5x106) were injected subcutaneously into both flanks of 8-12 week old female nude mice. Four mice were assigned to each group, no statistical method was used to predetermine sample size. The experiments were not randomized and the investigators were not blinded to allocation during experiments and outcome assessment. Tumor height and width were measured with a caliper every 2–3 days to calculate tumor volume (= width2 × height × 0.523). Mice were sacrificed 4 weeks post engraftment. All animal experiments were approved by the University of California, San Diego, Institutional Animal Care and Use Committee.

Policy information about studies involving human research participants

12. Description of human research participants

Describe the covariate-relevant population characteristics of the human research participants.

None